The Evolution of the Modified Compression Field Theory for Modeling Existing Concrete Structures: Field Assessment, Deterioration, and Repair

Anca Ferche¹ and Vahid Sadeghian²

¹Department of Civil, Architectural, and Environmental Engineering, University of Texas at Austin, TX, USA

²Department of Civil and Environmental Engineering, Carleton University, ON, Canada

Synopsis: Developed 40 years ago by Frank Vecchio and Michael Collins, the Modified Compression Field Theory (MCFT) and its successor, the Disturbed Stress Field Model (DSFM), have proven to be robust methodologies in modeling the response of concrete structures. Originally developed for newly designed concrete structures, they have been refined over the years to expand their applicability to various engineering problems, including modeling deteriorated and repaired structures. This paper reviews the evolution and application of MCFT in modeling and assessment of deteriorated and repaired concrete structures. The first part focuses on the application of MCFT to advanced field structural assessment, including stochastic analysis procedures that incorporate field data. The second part discusses the evolvement of MCFT to account for two of the most common deterioration mechanisms, reinforcement corrosion and alkali-silica reaction. The last part explores the application of the model to structures repaired with fiber-reinforced polymer composites. It is concluded that the extension of the MCFT formulation has enabled it to reliably predict the behavior of both deteriorated and repaired concrete structures.

<u>Keywords:</u> alkali-silica reaction, corrosion, fiber-reinforced polymer, modified compression field theory, nonlinear finite element analysis, structural assessment, strengthening and repair, stochastic simulation.

INTRODUCTION

From iconic landmarks that have stood the test of time to the everyday structures we rely on, concrete is an omnipresent material. Decades of infrastructure development have left us with an increasing number of aging and deteriorating reinforced concrete (RC) structures nearing the end of their service lives and requiring structural assessment. Managing this expanding stock of deteriorating concrete structures presents a significant challenge for the civil engineering community. Robust assessment tools are needed to critically evaluate the safety and serviceability of existing structures, prioritize necessary repairs, determine the most effective repair methods, and develop materials and design strategies for new or replacement structures. Timely and effective repair is essential for extending service life and ensuring safety. Repairing damaged elements can restore structural performance, enhance strength, ductility, and durability, and prevent further deterioration (Fig. 1). This approach not only maintains the structural functionality but also provides economic benefits by delaying the need for complete replacement. In the 21st century, advances in structural assessment—driven by innovations in modeling techniques and instrumentation—have revolutionized how we approach these issues. However, predicting the behavior of deteriorating concrete structures remains a complex challenge that requires advanced modeling approaches to account for diverse deterioration mechanisms and inform more effective repair strategies.

The design of new structures and the assessment of existing ones typically follow a limit state approach, primarily through cross-sectional analysis. This method evaluates the strength of an element relative to the internal actions generated by applied loads. In this approach, internal actions are derived from linear elastic analysis, while the member's strength is assessed based on the relevant limit state. This method relies on simplified assumptions regarding material constitutive models and the structural model. Despite these simplifications, it is highly efficient in the design phase of new structures, having been refined by committees worldwide and incorporated into design codes and guidelines (e.g., ACI 318, CSA A23.3, fib Model Code). When applying the same approach to existing structures affected by deterioration mechanisms or exhibiting various stages of distress, several of the assumptions made for newly designed structures become invalid. The constitutive models for materials such as concrete and steel reinforcement differ significantly when deterioration mechanisms are present. Additionally, a structural model based on linear elastic analysis is often inadequate. Linear elastic models assume that materials behave in a linear, elastic manner, which is no longer true for deteriorated materials. For example, concrete may exhibit nonlinear stress-strain behavior after cracking, and reinforcement may experience yielding due to corrosion. Moreover, deteriorated structures often develop cracks that alter stiffness and load distribution, which linear models cannot capture. To address these complexities and accurately assess the residual strength and deformation capacities of deteriorated RC structures, more advanced procedures are necessary. Nonlinear finite element analysis (NLFEA) has emerged as the most versatile and reliable approach, and its implementation for structural assessment is the focus of this paper, along with the evolvement of the Modified Compression Field Theory (MCFT) (Vecchio and Collins, 1986) in its application to existing, deteriorated, and repaired concrete structures.

Numerous diverse models and methodologies exist for the application of NLFEA to the structural assessment of sound concrete structures, ranging from smeared to discrete crack models, from fixed crack to rotating crack models, and from elasticity-based approaches to those based on plasticity and fracture mechanics. Smeared crack models, commonly employed in structural engineering, treat concrete as a quasi-continuous material, with cracks represented as average deformations distributed over an area. After cracking occurs, the concrete is considered an orthotropic material, with the effects of the cracks reflected in its stiffness, strength, and energy characteristics. Among the smeared crack models, the MCFT and its successor, the Disturbed Stress Field Model (DSFM) (Vecchio, 2000) have seen a broad range of applications, from design code implementation (e.g., AASHTO, CSA A23.3), to fiber-based modeling tools (e.g., Guner and Vecchio, 2010), to nonlinear finite element analysis (e.g., Vecchio, 2001).

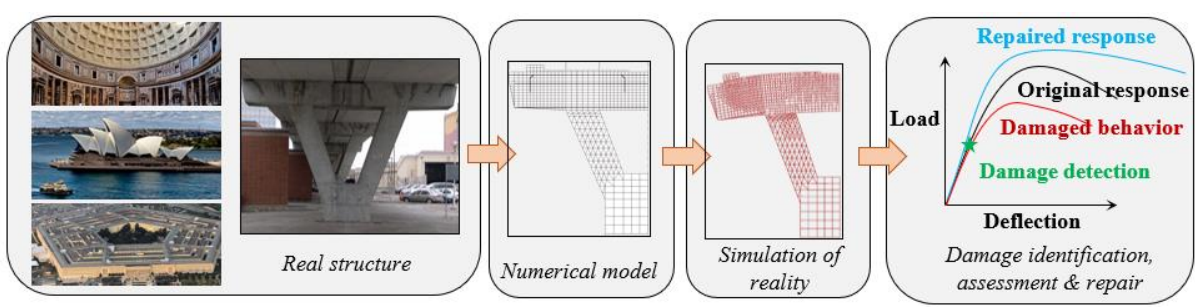


Figure 1 - The role of NLFEA in structural assessment

While initially developed for newly designed concrete structures, MCFT and the DSFM have been refined and extended over the years to address a wide range of engineering challenges, including the modeling of existing, deteriorated, and repaired structures. This paper examines the evolution and application of MCFT in the context of such structures. The first section explores the application of MCFT to advanced field structural assessment, including stochastic analysis methods that integrate field data. The second section highlights advancements in MCFT to address two prevalent deterioration mechanisms: reinforcement corrosion and alkali-silica reaction. Finally, the third section investigates the model's application to structures repaired using fiber-reinforced polymer composites. The findings demonstrate that the extended MCFT framework reliably predicts the behavior of both deteriorated and repaired concrete structures, confirming its adaptability and utility in diverse scenarios.

OVERVIEW OF THE MODIFIED COMPRESSION FIELD THEORY

The MCFT is an enhanced version of the original Compression Field Theory (CFT) (Mitchell and Collins, 1974), a smeared rotating crack model initially developed for analyzing shear and torsion in beams. Both models express compatibility, equilibrium, and constitutive relationships in terms of average stresses and strains. The CFT assumes that cracked concrete cannot resist tension, with the shear force carried by a diagonal compression field. The inclination of this compression field is determined similarly to the Tension Field Theory (Wagner, 1929), which addresses post-buckling shear resistance in thin metal girders. The MCFT improves upon the CFT by considering key factors such as the reduction in compressive strength due to transverse cracking, the residual tensile strength of concrete after cracking, and local stress conditions at the crack surface. It forms the basis of shear design provisions in the Canadian design code (CSA A23.3-24) and the AASHTO LRFD Bridge Design Specifications (AASHTO, 2024). Further advancements were made when Vecchio (2001) introduced the Disturbed Stress Field Model (DSFM), which addressed some of the MCFT's limitations and improved model accuracy. The most noticeable changes included allowing the orientation of principal stresses to deviate from that of principal strains, incorporating deformations due to crack slip in the compatibility relationships, and removing the shear stress check along the crack required by the MCFT. Bentz et al. (2006) later simplified the MCFT to develop closed-form equations for predicting the shear strength of RC members suitable for implementation in design codes.

Figure 2 compares the equilibrium, compatibility, and constitutive relationships across the CFT, MCFT, and DSFM. The formulation of the models along with the constitutive relations commonly used with them have been documented in literature (Wong et al., 2013; Sadeghian and Vecchio, 2018). In the following, an overview of the formulation is presented to provide the necessary background for understanding the application of the models to analysis of deteriorated and repaired concrete structures.

The total strains in concrete can be expressed as a summation of: 1) net strains, $\{\varepsilon_c\}$, 2) elastic offset strains, $\{\varepsilon_c^o\}$ (e.g., thermal effects, shrinkage strains, ASR expansion, prestrains, and lateral expansion due to Poisson's effects), 3) plastic offset strains, $\{\varepsilon_c^p\}$ (permanent deformation resulting from loading history), and 4) crack slip offset strains, $\{\varepsilon_c^s\}$ (due to shear slip on the crack surface). The total concrete strains can be written as:

$$\{\varepsilon\} = \{\varepsilon_{c}\} + \{\varepsilon_{c}^{0}\} + \{\varepsilon_{c}^{p}\} + \{\varepsilon_{c}^{s}\} \tag{1}$$

By transferring concrete strains from the global coordinate system to the principal directions (ε_{c1} , ε_{c2}), concrete principal stresses (f_{c1} , f_{c2}) can be calculated using the constitutive models implemented into the MCFT and DSFM models. Wong et al. (2013) provided a comprehensive summary of these constitutive models. Knowing the strains and stresses in the principal directions, the secant moduli representing the stiffness of concrete material are determined as follows:

$$\overline{E}_{c1} = \frac{f_{c1}}{\varepsilon_{c1}} \quad ; \quad \overline{E}_{c2} = \frac{f_{c2}}{\varepsilon_{c2}} \quad ; \quad \overline{G}_{c} = \frac{\overline{E}_{c1} \cdot \overline{E}_{c2}}{\overline{E}_{c1} + \overline{E}_{c2}}$$
 (2)

where \bar{E}_{c1} and \bar{E}_{c2} are the normal secant moduli in principal directions 1 and 2, respectively, and \bar{G}_c is the shear secant modulus. Considering concrete as an orthotropic material with Poisson's effects represented as elastic offsets, the stiffness matrix of concrete in the principal directions can be expressed as:

$$[D_c]' = \begin{bmatrix} \bar{E}_{c1} & 0 & 0\\ 0 & \bar{E}_{c2} & 0\\ 0 & 0 & \bar{G}_c \end{bmatrix}$$
 (3)

A similar approach can be applied to determine the local stiffness matrix of the reinforcement. The total strains in the reinforcement can be represented as a summation of: 1) net strains, $\{\epsilon_s\}$, 2) elastic offset strains, $\{\epsilon_s^o\}$ (thermal and prestrain effects), and 3) plastic offset strains, $\{\epsilon_s^p\}$ (due to steel yielding and damage resulted from loading history). The total strains in the ith reinforcement component can be written as:

$$\{\varepsilon\}_{i} = \{\varepsilon_{s}\}_{i} + \{\varepsilon_{s}^{0}\}_{i} + \{\varepsilon_{s}^{p}\}_{i} \tag{4}$$

The secant modulus of the ith reinforcement component and its stiffness matrix in the longitudinal direction of the reinforcement can be defined as:

$$\overline{E}_{si} = \frac{f_{si}}{\varepsilon_{si}} \quad ; \quad [D_s]_i' = \begin{bmatrix} \rho_i \overline{E}_{si} & 0 & 0\\ 0 & 0 & 0\\ 0 & 0 & 0 \end{bmatrix}$$
 (5)

where ρ_i is the reinforcement ratio of the ith reinforcement component. This equation accounts for the uniaxial resistance of the reinforcement. The shear resistance of the reinforcement is considered using dowel models adopted from the literature. Also, the formulation assumes the total strains developed in the reinforcement and the concrete are equal at the same location (i.e. a perfect bond between the reinforcement and the concrete). The bond-slip behavior between material components can be modeled using interface elements which will be discussed in more detail later in the paper.

After determining the local stiffness matrices of the concrete and reinforcement, they can be transformed to the global coordinate system:

$$[D_c] = [T_c]^T [D_c]' [T_c] \qquad ; \qquad [D_s]_i = [T_s]_i^T [D_s]_i' [T_s]_i$$
(6)

where $[T_c]$ is the concrete transformation matrix defined based on the direction cosines relating the principal directions to the global directions, and $[T_s]$ is the steel transformation matrix defined based on the direction cosines relating the longitudinal reinforcement direction to the global directions. Using the superposition principle, the stiffness matrix of a reinforced concrete material with "n" reinforcement components can be expressed as:

$$[D] = [D_c] + \sum_{i=1}^{n} [D_s]_i$$
 (7)

Knowing the composite stiffness matrix, the total stresses can be related to the total strains as follows:

$$\{\sigma\} = [D]\{\epsilon\} - \{\sigma^0\} \tag{8}$$

where $\{\sigma^0\}$ is the pseudo-stress vector defined to account for stresses corresponding to strain offsets, ensuring that external stresses applied to an element result only in net strains.

$$\{\sigma^{o}\} = [D_{c}](\{\varepsilon_{c}^{o}\} + \{\varepsilon_{c}^{p}\} + \{\varepsilon_{c}^{s}\}) + \sum_{i=1}^{n} [D_{s}]_{i}(\{\varepsilon_{s}^{o}\}_{i} + \{\varepsilon_{s}^{p}\}_{i})$$

$$(9)$$

Using the composite material stiffness matrix, the stiffness matrix of the RC element can be determined:

$$[k] = \int_{\text{vol}} [B]^{\text{T}}[D][B] dv \tag{10}$$

where [B] is the strain-displacement matrix defined based on the shape of the element. By assembling the stiffness matrices of all elements, the global stiffness matrix can be calculated to relate nodal forces and displacements in a FE model.

SP-365: Modeling and Performance Assessment of Concrete Structures

	Compression Field Theory (CFT)		Modified Compression Field Theory (MCFT) – Original Formulation		Disturbed Stress Field Model (DSFM)		
Equilibrium	Average stresses perpendicular to crack f_{sy} f_{c2} f_{sx} y T_{xy} T_{xy}	Average stresses parallel to crack	Average stresses parallel to crack	Local stresses along crack surface Ox Txy Vci Crack Crack Crack Txy X	Average stresses perpendicular to crack f_{sj} τ_{xy} τ_{xy}	Average stresses parallel to crack σ_{x} τ_{xy} σ_{x}	Local stresses along crack surface
	↓σ _y Local stress condition	$\downarrow \sigma_y$ ons are not considered	↓o _y For average stress perp	↓σ _y pendicular to crack see CFT	$\downarrow \sigma_{y}$ Unlike MCFT, the	↓σ _y re is no shear stress limit	$\mathbf{\downarrow \sigma_y}$ t on the crack surface
Compatibility	Average strain conditions ε_{cy} $\frac{y}{1}$ $\frac{y}{2}$ 1 ε_{cx} 1 ε_{cx} 1 ε_{cx} 1 ε_{cx}		v_{ci} f_{ci} v_{ci} f_{ci} v_{ci} f_{ci} v_{ci} f_{ci} f		$\begin{array}{cccccccccccccccccccccccccccccccccccc$		
	Slip deformations are not considered		Average strain conditions are similar to CFT Slip deformations are not considered		Average strains Slip strains Total strains $\theta_{\epsilon} \neq \theta_{\sigma}$		
Constitutive Relationships	Concrete in tension f_{c1} f_{cr} $f_{c1} = 0$ ϵ_{cr} ϵ_{c1}	Concrete in compression $f_{c2} \oint f_{c2max} = f'_c$	Tension stiffening f_{c1} f_{cr} \overline{E}_{c1} \overline{E}_{c1}	Compression softening f_{c2} f'_{c} f_{c2}	Tension soften f_{c1}^a f_{cr} \overline{E}_{c1} ε_{cr}	f _{c1} f _{cr}	Tension stiffening $\frac{1}{\overline{E}_{c1}}$ ε_{cr} ε_{c1}
	Reinforcement response f_s f_y ε_y ε_s		Shear stress on crack $ \begin{array}{c c} & 1.0 \\ \hline & 1.0 \\ \hline & f_{ci}/v_{cimax} \end{array} $	Reinforcement response f_s f_y \overline{E}_s ε_y ε_s	Compression softe f_{c2} f'_{c} f_{p} \overline{E}_{c2} $\varepsilon_{p} \varepsilon'_{c}$	c2 .	$\begin{array}{c c} \text{nforcement response} \\ \hline f_s \\ \hline \\ \overline{E}_s \\ \hline \\ \varepsilon_y \ \varepsilon_{sh} \ \varepsilon_u \\ \end{array}$

Figure 2 - Comparison between CFT, MCFT, and DSFM models (Sadeghian and Vecchio, 2018)

APPLICATION OF MCFT TO ADVANCED STRUCTURAL ASSESSMENT

Over the years, various MCFT-based approaches have been developed to support structural assessment. These range from sectional analysis methods grounded in the simplified MCFT (Bentz et al., 2006; Bentz, 2010), to crack-based assessment techniques (Zaborac et al., 2019) and NLFEA procedures (Vecchio, 2001). The following sections provide an overview of the use of MCFT-based NLFEA tools in the context of structural assessment. The development and application of such tools have been significantly influenced by Frank Vecchio at the University of Toronto. In his course, CIV1163 Mechanics of Reinforced Concrete, Vecchio brought together theoretical principles and practical applications to teach structural assessment and forensic analysis. He focused on evaluating the safety, performance, and intervention needs for concrete structures, emphasizing the importance of robust simulations. He also emphasized caution in using these tools, as reflected in the Memorandum of Understanding that every student in the course had to sign: "The analysis methods and software introduced in this course are merely tools. A tool in the hands of Michelangelo will create a masterpiece; a tool in the hands of a novice may yield a mess. No two artists will arrive at the same result."

Vecchio's emphasis on the limitations and capabilities of analysis tools resonates with the growing application of NLFEA in structural assessment. As these tools continue to evolve, their versatility and depth of insight have led to their increasing use in assessing existing structures, analyzing failed or distressed systems, exploring repair and rehabilitation strategies, and optimizing design for more efficient solutions. NLFEA not only provides insights into the inherent strength or safety margins of a structure but also helps determine critical factors such as the mode of failure and energy absorption capacity. Additionally, these procedures enable a detailed investigation of the mechanisms governing structural behavior. Despite their potential, NLFEA programs for design and analysis of concrete structures face challenges in achieving a level of maturity where users can reliably develop geometric models, define basic material parameters, and predict structural responses—such as capacity, deformation, and stress distribution—under various loading conditions.

Vecchio's teaching reinforced the importance of ensuring that simulation outcomes inform decision-making effectively. He emphasized that analysts must produce credible and defensible results, which requires a technically sound and transparent approach. This includes a clear understanding of the modeling assumptions, limitations, and deficiencies, as well as the modeling requirements. Furthermore, he underscored the critical role of verification and validation activities, ensuring that simulations were supported by rigorous testing and data-driven insights. Commonly, there are two approaches to the assessment of the strength and behavior of structures:

- One option the analyst has is to apply material strength reduction factors and load amplification factors. The goal is to demonstrate that the structure can fully withstand the applied factor loads without collapse. As long as the NLFEA converges to a stable solution and the structure does not fail, regardless of the extent of damage or distress, the structure is considered to satisfy the code's strength requirements. However, critics of this method argue that applying different material and load factors may alter the nature of the behavior or the failure mode. Additionally, this procedure may not accurately reflect the conditions at service load levels, though it remains useful for correlating observed damage with the predicted response.
- Alternatively, the analyst can use unfactored material properties and design loads in the model. The load is then gradually increased in fixed proportions until the structure reaches failure, resulting in the determination of the ultimate load factor. The ultimate load factor is subsequently compared to a target safety factor to ensure the structure's adequacy. This approach provides a direct assessment of the structure's load-carrying capacity by evaluating its behavior under progressively increasing loads, ensuring that it can withstand forces beyond typical design loads while maintaining a safety margin. The challenge lies in determining the appropriate global safety factor, which depends on factors such as the proportion between dead load and live load, the type of failure (e.g. ductile or brittle), and the specific code being followed.

In the calculation of the global safety factor, consideration should be given to the bias factor of the NLFEA software used, as it directly impacts the reliability of the analysis. For example, Vecchio et al. (2001) employed MCFT-based FE models and reported mean calculated-to-experimental strength ratios (bias factors) of 1.000, 1.011, and 1.022 for beams, shear walls, and panels, respectively, with coefficients of variation of 5.3%, 20.3%, and 9.6%. Similarly, Hunter et al. (2021a) analyzed 318 shear-critical beams without transverse reinforcement and found a bias factor of 1.106 with an 18.3% coefficient of variation. These findings underscore the variability of bias factors across different structural elements, emphasizing the need for rigorous evaluation of the performance of analysis software.

This evaluation should be conducted through validation studies pursued in a hierarchical manner, progressing from material-level characterization to element-level and structural-level benchmark tests, as illustrated in Fig. 3 and recommended in the fib Practitioners Guide to FE Modeling of RC Structures (2008). Element-level benchmark tests on panel elements under biaxial stress state including combinations of normal and shear stresses should be used to evaluate the capability of the methodology employed to model influential aspects of the biaxial response. These aspects include shear transfer across the cracks, compression softening, tension stiffening, and the influence of compression stresses on crack width and crack spacing. Subsequently, relevant structural-level benchmark tests should be used to validate the approach through comparisons of performance metrics such as initial stiffness, strength, deformations, overall load-displacement response, reinforcement strains, crack width and crack spacing.

By systematically comparing predicted-to-experimental response parameters across various performance metrics, the validation study serves to determine the bias factor, which reflects the software's ability to model real-world behavior. The bias factor informs the adjustment of analysis results to account for any systematic overestimation or underestimation. In this process, a normal distribution is generally assumed for the experimental-to-calculated strength ratios and the global safety factor is calculated adopting a threshold for the cumulative distribution function.

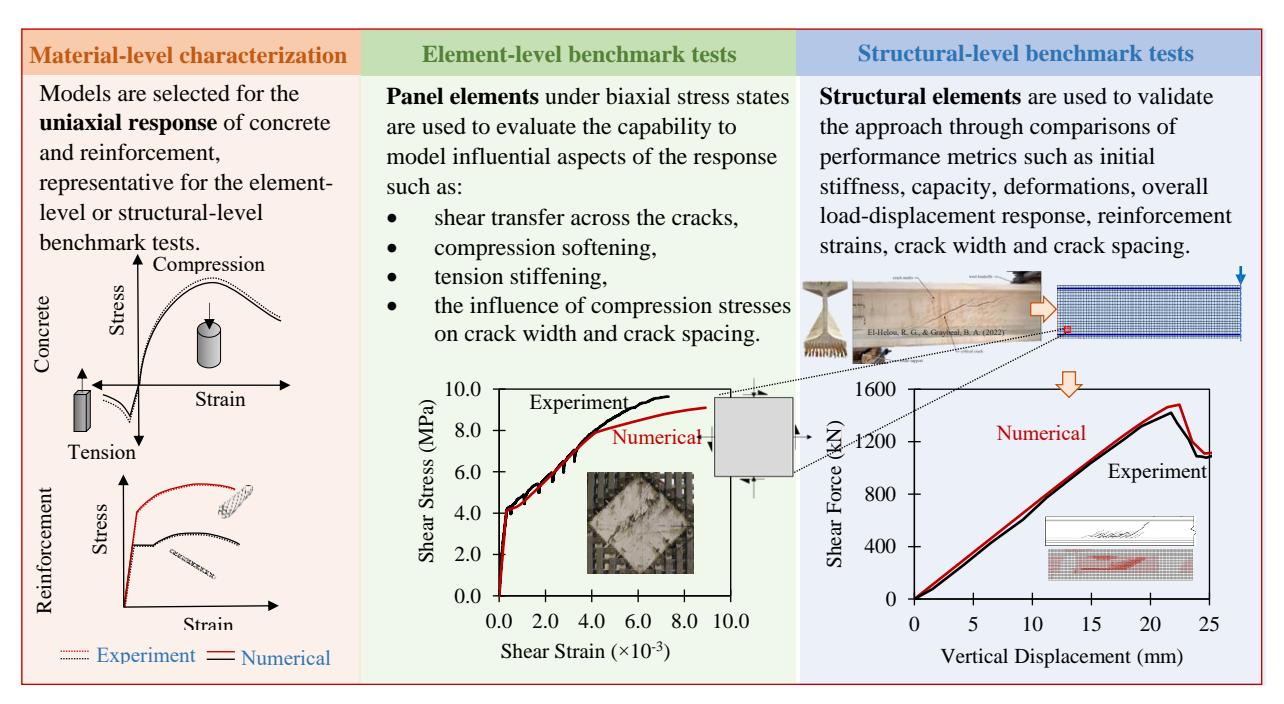


Figure 3 - Hierarchical validation study for structural assessment

MCFT-based tools have evolved significantly to address the uncertainties inherent in structural assessment. One notable advancement was the integration of stochastic analysis into NLFEA programs such as VecTor2 (Wong et al., 2013). Unlike traditional deterministic methods, which cannot account for the variability in material properties and their impact on structural behavior, stochastic simulations incorporate established material distributions and damage prediction models to provide a more comprehensive understanding of structural performance. Research demonstrated that stochastic analysis could adequately replicate experimental results while offering a confidence level for each specimen, surpassing the limitations of deterministic approaches (Hunter et al., 2021a and 2021b; Ma, 2018).

Hunter et al. (2021a) reported the stochastic simulation results of four beam specimens without transverse reinforcement with depths ranging from 500 mm (19.7 in.) to 4000 mm (157.5 in.), tested at the University of Toronto. Each simulation consisted of a random field using Latin hypercube sampling for the specified concrete strength of 30 MPa (4350 psi). The steel properties were assumed to be deterministic, primarily because the mechanical properties of the longitudinal reinforcement have limited influence on the behavior of shear-critical beams with no transverse reinforcement. Additionally, the strain in the steel is a function of the modulus of elasticity, which generally exhibits only small variability. The spatial variation of the concrete properties due to the random fields was based on the measured properties of specimen PLS4000 tested by Collins et al. (2020). A correlation length of 1200 mm (47.2 in.) and the random field coefficient of variation of 5.0% were selected.

For each beam, the simulation results produce a series of load-deflection curves. A typical plot of the stochastic simulation results is shown in Fig. 4(a). The peak loads obtained from the stochastic simulations can then be analyzed as a set of random data. A statistical distribution is fitted to the results of each simulation. Fig. 4(b) shows an example of the distribution of the peak load for specimen YB2000. The results of each simulation were determined to be normally distributed. Each of the stochastic simulations showed a mean value close to the nominal resistance calculated by the General Shear Design Method of CSA A23.3-24 (CSA, 2024). A plot of the General Method compared with the stochastic simulation results is presented in Fig. 5, where the simulation results were transformed from applied peak load to shear force per meter.

Further advancements by Ma (2018) explored the incorporation of early-stage field measurements, such as deflections, crack widths, and reinforcement strains, to recalibrate stochastic outputs. This recalibration methodology narrowed confidence intervals, enhancing the accuracy of predictions. Such applications highlight the potential of stochastic analysis as a practical tool for field assessments, enabling more reliable evaluations of structural performance and safety. In real-world assessment scenarios, where response results are often unknown and subject to uncertainties, this approach provides a significant advantage. By utilizing actual damage measurements, it allows for the refinement of predictive models based on real-time data, improving the reliability of the assessment process. This methodology offers a more robust framework for evaluating structures in service, where traditional deterministic models may not fully capture the complexities of actual conditions.

In addition to the inherent variability of concrete and steel material properties in existing structures, engineers must often consider the effects of various deterioration mechanisms and their impact on structural behavior. Over time, MCFT-based software tools have been enhanced to address two of the most prevalent deterioration mechanisms: corrosion of reinforcing bars and alkali-silica reaction (ASR). The following sections provide a summary of these advancements and their implications for structural assessment.

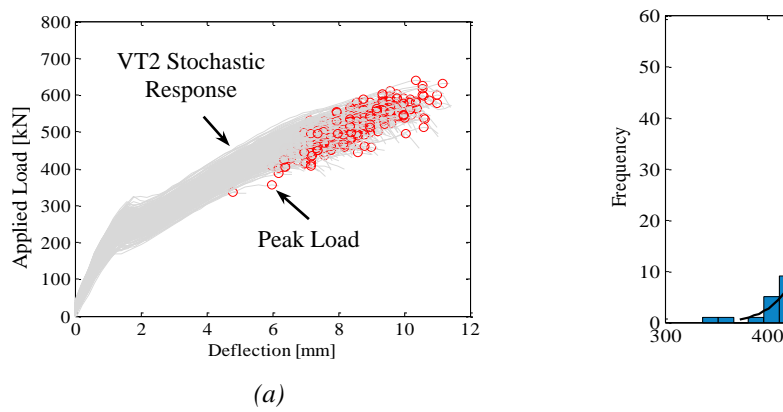


Figure 4 - Example of stochastic simulation results for specimen YB2000: (a) Simulated load-deflection and (b) Statistical distribution of peak load. (Hunter et al. 2021a) (Note: 1.0 mm = 0.04 in., 1 kN = 0.225 kip.)

500

Peak Load [kN]

600

700

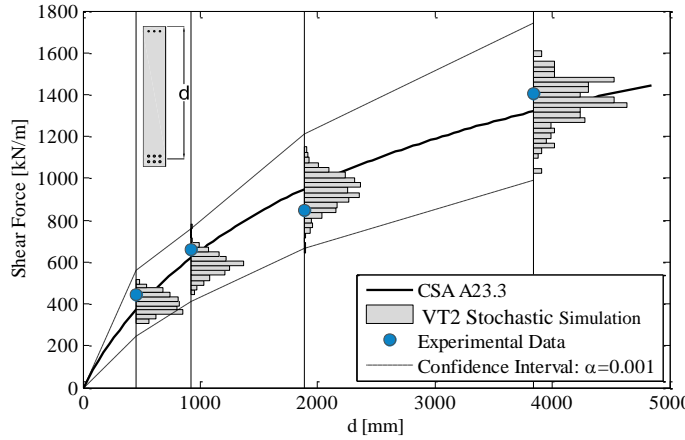


Figure 5 - Comparison of results obtained from stochastic simulation, experimental tests, and CSA-A23.3. (Hunter et al. 2021a) (Note: 1.0 mm = 0.04 in., 1 kN = 0.225 kip.)

APPLICATION OF MCFT TO MODELING CORROSION-DAMAGED RC STRUCTURES

Corrosion of reinforcement can manifest in two forms, as shown in Fig. 6: uniform and pitting corrosion. Uniform corrosion occurs evenly across the surface of the reinforcing bar leading to a gradual reduction in cross-sectional area, while pitting corrosion is characterized by localized areas of degradation resulting in deep pits in the reinforcing bar. Both forms of corrosion can significantly affect the durability of RC members by reducing the cross-sectional area of the reinforcement, deteriorating the bond between the reinforcement and the concrete, degrading the mechanical properties of the reinforcement, and causing concrete cracking near the corroded reinforcement. All these mechanisms are influenced by the depth of corrosion penetration, which is directly proportional to the corrosion rate. The corrosion rate is typically defined as the loss of metal per unit of surface area per unit of time (mm/year) or as current density $(1\mu A/cm^2)$. As such, in all modeling approaches, the corrosion rate and the depth of corrosion penetration serve as key input parameters. Various models are available in the literature to characterize the implications of corrosion on RC members, such as those developed by Alonso et al. (1988) and Liu and Weyers (1998) for the reduction in the cross-sectional area of the reinforcement, Stewart and Al-Harthy (2008) for pitting (localized) corrosion, Chung et al. (2008) and Feng et al. (2016) for bond strength deterioration, Pantazopoulou and Papoulia (2001) and Wang and Liu (2004) for concrete cover cracking, and Cairns et al. (2005) for the deterioration of the mechanical properties of the reinforcement. These behavioral models have been implemented in various nonlinear analysis procedures to assess the response of corrosion-damaged RC structures. Kashani et al. (2019) reviewed and evaluated several of these analytical models.

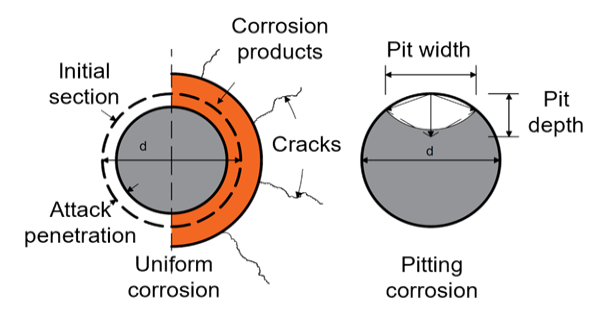


Figure 6 - Comparison of uniform and pitting corrosion in RC members

Modeling methodology

The following summarizes the models and formulations implemented in VecTor2, a 2D nonlinear FE software developed based on MCFT, to account for the effects of both uniform and pitting corrosion on RC members. For more information about the formulations and verification analyses refer to Habibi et al. (2022).

Corrosion rate - Two models were considered for determining the corrosion rate and the reduction in the cross-sectional area of a corroded rebar. The first model, proposed by Alonso et al. (1988), is based on Faraday's law which relates the mass loss due to corrosion to the current produced by anodic areas. According to this model, the corrosion rate, $\frac{dr_b}{dt}$, and the remaining diameter of a corroded rebar, $d_b(t)$, can be expressed as:

$$\frac{dr_b}{dt} = 0.0116i_{cor} \left(\frac{mm}{year}\right) \tag{11}$$

$$d_b(t) = d_{bo} - 0.0232i_{cor}.t \quad (mm)$$
(12)

where i_{cor} is the corrosion current density in ${}^{\mu A}/_{cm^2}$, d_{bo} is the initial bar diameter in mm, and t is the period of effective corrosion in years.

The second model, proposed by Liu and Weyers (1998), expresses the rate of corrosion in terms of the growth rate of rust products, which is inversely proportional to the ionic diffusion distance. In this model, after determining the weight of the produced rust, the weight of the consumed steel is calculated using the ratios of the molecular weight of common types of rust to that of iron. Habibi et al. (2022) compared the predictions of the Alonso et al. (1988) model and the Liu and Weyers (1998) model against experimental results obtained from accelerated corrosion tests on beams and prisms available in the literature. They concluded that the Alonso et al. (1988) model which accounts for the duration of the corrosion is more accurate and subsequently implemented it into VecTor2. To account for pitting

corrosion, the model proposed by Stewart and Al-Harthy (2008) was adopted to calculate the cross-sectional area of the pit (i.e. the reduction in the area of rebar) in terms of the maximum pit depth and the initial bar diameter.

Cover cracking - Corrosion induced-cracking is modeled by calculating initial strains generated in the element in the vicinity of a corroded reinforcing bar. Given that the induced cracks are in the radial direction (see Fig. 7), the strain components should be represented with respect to the polar coordinate system:

$$\varepsilon_r = \frac{\partial u_r}{\partial r} \; ; \; \varepsilon_\theta = \frac{u_r}{r} + \frac{\partial u_\theta}{r \partial \theta}$$
 (13)

where ε_r and ε_θ are the radial and tangential strains, u_r and u_θ are the radial and tangential displacements, and r is the radial distance from the center of the reinforcing bar. Assuming that deformations due to corrosion along the z-axis are negligible and that the tensile stresses developed around the reinforcing bar are symmetrical and independent of the angle θ , it can be shown that the shear strain components are insignificant and thereby ε_r and ε_θ are the principal strains (ε_1 , ε_2). After transferring the principal strains into the global coordinate system, they can be incorporated into the MCFT formulation as prestrains contributing to the pseudo-stress vector expressed in Eq. 9.

$$\{\varepsilon_{c}^{cor}\} = \begin{cases} \varepsilon_{x} \\ \varepsilon_{y} \\ \gamma_{xy} \end{cases} = \left\{ \varepsilon_{1} \sin^{2}(\theta + \frac{\pi}{2}) + \varepsilon_{2} \cos^{2}(\theta + \frac{\pi}{2}) \right\}$$
(14)

$$\{\sigma^{o}\} = [D_{c}](\{\varepsilon_{c}^{o}\} + \{\varepsilon_{c}^{p}\} + \{\varepsilon_{c}^{s}\} + \{\varepsilon_{c}^{cor}\}) + \sum_{i=1}^{n} [D_{s}]_{i}(\{\varepsilon_{s}^{o}\}_{i} + \{\varepsilon_{s}^{p}\}_{i})$$

$$(15)$$

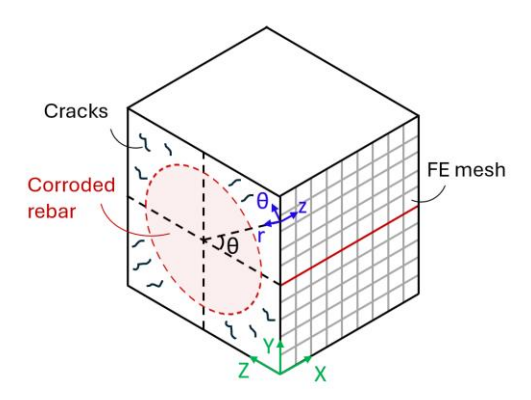


Figure 7 - Polar and cartesian coordinate systems used to calculate corrosion induced-cracking in VecTor2

Two models were implemented in VecTor2 to calculate the radial and tangential strains due to cracking in the concrete cover (ε_r , ε_θ). The first model, developed by Wang and Liu (2004), represents the concrete cover as two thick-wall cylinders subjected to unform internal pressure. As the corrosion rate increases, the inner cylinder cracks while the outer one is assumed to remain uncracked. The cracking of the inner cylinder is modeled using a tensile stress-strain relationship in the tangential direction, which consists of a linear elastic pre-peak response followed by a bilinear softening branch, calculated based on fracture energy. The second model, proposed by Pantazopoulou and Papoulia (2001), employs a finite difference approach to capture the cracking of concrete cover. In this approach, the cover thickness is discretized into a number of segments, and each segment is analyzed by solving the differential equation of a hollow cylinder under uniform internal pressure, expressed as a function of stresses and strains in the polar coordinate system. Habibi et al. (2022) compared the predictions of the Wang and Liu (2004) model and the Pantazopoulou and Papoulia (2001) model for an 8 mm (0.31 in.) reinforcing bar with a clear concrete cover of 76 mm (2.99 in.) that experienced a corrosion rate of 20.9 mm/year (0.82 in/year). While both models predicted similar pressure buildup values around the rebar, the Wang and Liu (2004) model underestimated both the radius of cracked concrete and the surface strain induced by corrosion.

Bond strength - The bond strength between steel and concrete is provided by adhesion, friction, and the bearing of rebar deformations on the concrete. However, the buildup of flaky corrosion products around the rebar significantly reduces both adhesion and friction. In addition, corrosion-induced cracking weakens the ability of concrete to confine the reinforcement. Consequently, the bond between a corroded reinforcing bar and concrete can experience substantial degradation, negatively impacting the performance of the structural member.

In VecTor2, the bond-slip behavior is modeled by using link elements that connect the reinforcement to the concrete elements. The bond-slip relationship can be defined by either choosing one of the bond models available in the software or manually specifying a multi-segment linear response. To account for the reduction in bond strength due to corrosion, four models were incorporated into the software. Some models were calibrated based on experimental data (e.g., Chung et al. 2008), while others were derived from numerical analysis (e.g., Feng et al. 2016). Each model calculates a reduction factor for the bond strength of corroded rebar, with the extent of damage typically measured by the weight loss of the rebar due to corrosion. Through a verification study, Habibi et al. (2022) suggested using the model by Chung et al. (2008) as it provided more conservative predictions.

Mechanical properties - To account for the effects of pitting corrosion on the mechanical properties of the reinforcement, the following equations were used to adjust the yield strength (f_y) , ultimate strength (f_u) , and the strain corresponding to the ultimate strength (ε_u) of the reinforcement:

$$f_y = (1 - \alpha_y Q_{cor}) f_{yo} \quad ; \quad f_u = (1 - \alpha_u Q_{cor}) f_{uo} \quad ; \quad \varepsilon_u = (1 - \alpha_1 Q_{cor}) \varepsilon_{uo}$$
 (16)

where f_{yo} , f_{uo} , and ε_{uo} are the yield strength, ultimate strength, and ultimate strain of a non-corroded bar, respectively; Q_{cor} is the percentage of the cross-section loss; and α_y , α_u , and α_1 are empirical coefficients taken from a study by Cairns et al. (2005).

Verification studies

Habibi et al. (2022) conducted a comprehensive set of deterministic and stochastic analyses to evaluate the accuracy of the proposed modeling methodology for corrosion-affected RC members. The deterministic analyses included modeling 49 RC beam specimens collected from three different experimental programs, with varying degrees of reinforcement corrosion, geometric dimensions, reinforcement ratios, and loading conditions. The stochastic analyses were performed to account for irregularity and heterogeneity of both uniform and pitting corrosion observed in the tests, treating the corrosion rate either as a single random variable or as a random field to consider spatial variability. An example of each type of analysis is provided in the following.

Deterministic modeling - Maaddawy et al. (2005) tested a series of identical RC beams under a four-point loading condition after 50, 110, 210, and 310 days of accelerated corrosion. As shown in Fig. 8, only the middle portion of the tension reinforcement was exposed to chloride, while the remaining length was protected by an epoxy coating. Habibi et al. (2022) created a FE model of each specimen in VecTor2 with an element size of approximately 25 mm × 25 mm (see Fig. 8). Concrete was modeled using rectangular elements, while truss elements were used for longitudinal and transverse reinforcements. Link elements were placed between concrete elements and tension reinforcement elements to capture bond-slip behavior. The corroded steel material type was assigned to the portion of the tension reinforcement exposed to chloride, while the normal steel material was selected for the remining reinforcing bars.

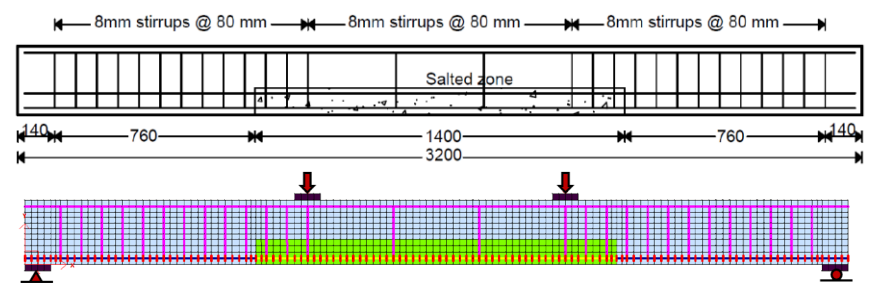


Figure 8 - Elevation view of Maaddawy et al. (2005) beam specimens and FE model in VecTor2 (Habibi et al. (2022)) (Note: 1.0 mm = 0.04 in.)

Figure 9 compares the experimental and numerical load-deflection responses as well as the crack widths along the middle portion of the beam exposed to chloride. It can be seen that the model was able to capture the experimental behavior with good accuracy. There was a tendency to overestimate the ductility capacity of the beams, which may be attributed to the underestimation of the effect of pitting corrosion, particularly for specimens exposed to longer periods of corrosion.

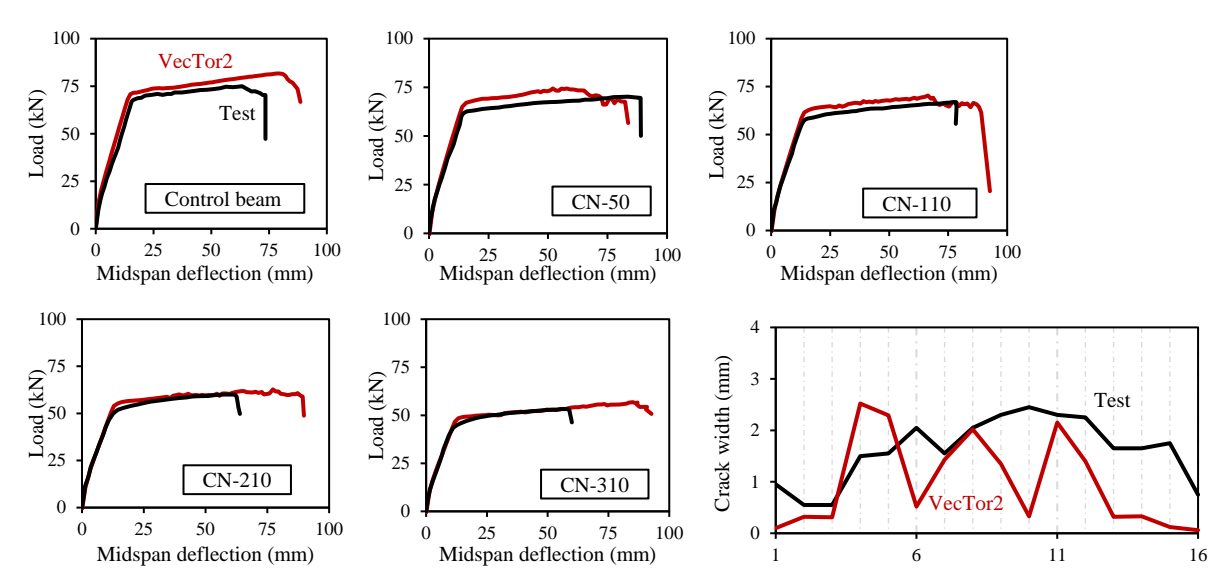


Figure 9 - Comparison of experimental and numerical load-deflection responses and corrosion-induced cracking near the midspan of Maaddawy et al. (2005) beam specimens (Habibi et al. (2022)) (1.0 mm = 0.04 in., 1 kN = 0.225 kip.)

Stochastic modeling - Habibi et al. (2022) extended the stochastic analysis framework developed by Hunter et al. (2021) to incorporate uncertainties associated with corrosion. To model uniform corrosion, the corrosion rate was treated as a random variable with a lognormal probability distribution obtained from curve fitting to experimental data collected from the literature. The spatial variability of corrosion was considered by constructing an empirical semivariogram for each realization of the data field. Stochastic simulations with 100 samples were performed on the Maaddawy et al. (2005) beam specimens. Although the average ultimate load was in good agreement with the experimental results, there was considerable variability in the predicted ductility. It was found that the COV of the ultimate load and displacement increased substantially with corrosion time. However, the impact of the spatial variability of corrosion was found to be insignificant.

The randomness due to pitting corrosion was modeled using a Gumbel distribution proposed by Stewart and Al-Harthy (2008) based on statistical analysis of maximum pit depth measured from corroded reinforcing bars. In the FE model, a random pitting factor was generated for every corroded truss element which was then used to calculate the cross-sectional loss and degradation in material properties based on the formulations discussed in the previous section. Figure 10 shows the stochastic simulation results for one of the beam specimens tested by Maaddawy et al. (2005). The variability in the ultimate load and ductility was more significant than that obtained from simulations based on uniform corrosion. It was found that as the maximum pitting factor increased, the ultimate load and ductility decreased.

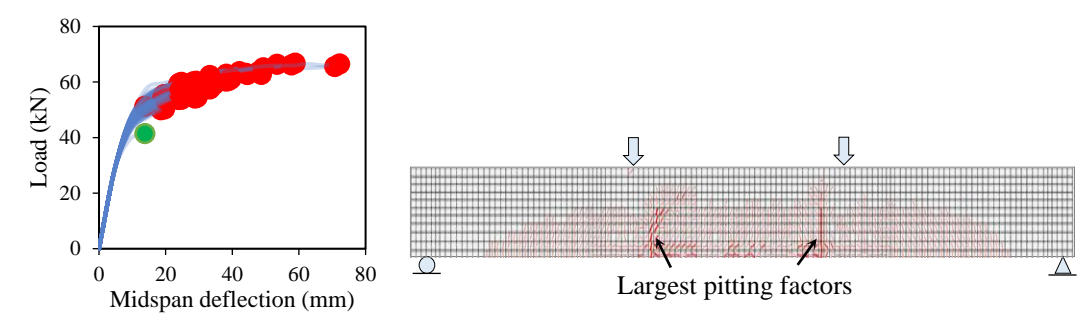


Figure 10 - Load-deflection responses and crack patterns obtained from stochastic simulations of pitting corrosion in CN-110 specimen (Habibi et al. (2022)) (Note: 1.0 mm = 0.04 in., 1 kN = 0.225 kip.)

APPLICATION OF MCFT TO MODELING ASR-AFFECTED STRUCTURES

The most common endogenous chemical reaction affecting existing concrete structures is the alkali-silica reaction (ASR), a chemical reaction between alkali hydroxides from the cement paste and certain siliceous minerals in the aggregates. This reaction produces a gel that swells in the presence of moisture, leading to pressure buildup, macroscopic expansion, and cracking. ASR impacts structural behavior through mechanisms that render conventional linear-elastic analyses inadequate. The induced expansion, heavily influenced by long-term stress levels and internal and external restraints, is accompanied by a degradation in concrete's mechanical properties, including compressive and tensile strengths, Young's modulus, and Poisson's ratio.

Several semi-empirical numerical constitutive models have been developed to capture the effects of ASR at different scales, ranging from material to structural levels. These models are typically categorized into three types based on the modeling scale: micro-models, meso-models, and macro-models. Micro-models primarily focus on the chemical and physical processes occurring at the microscopic level, specifically targeting the transport equations of reactants and diffusion processes. Meso-models operate at a scale ranging from 1.0 to 10.0 cm (0.39 to 3.94 in.), emphasizing the heterogeneous nature of concrete. This approach is particularly useful for understanding how ASR-induced expansions affect concrete at a more granular level. Macro-models, which are the focus of this work, are suited for assessing the global behavior of a structure or a member. Unlike micro and meso-models, macro-models prioritize the overall structural response to ASR effects, considering how these reactions influence the integrity and performance of the structure as a whole. This approach enables the analysis of large-scale structural systems and provides insights into the long-term implications of ASR.

Ferche et al. (2017) developed a two-stage analysis procedure for the assessment of ASR-affected RC members, summarized in Fig. 11, compatible with MCFT. The procedure was incorporated in VecTor2 and VecTor3. The first stage involves the assessment of ASR-induced expansion and the deterioration of concrete mechanical properties under long-term loading. The expansion is greatly influenced by the stress level and so, at this phase, the loads applied to the structure should be sustained loads only. In order to evaluate the residual capacity of the structural elements, the second stage of the simulation involves a nonlinear analysis that accounts for the stress condition and cracking obtained from Stage 1. An overview of the formulations used for the calculation of the ASR-induced expansion and consideration of the changes in the mechanical properties of concrete is presented below.

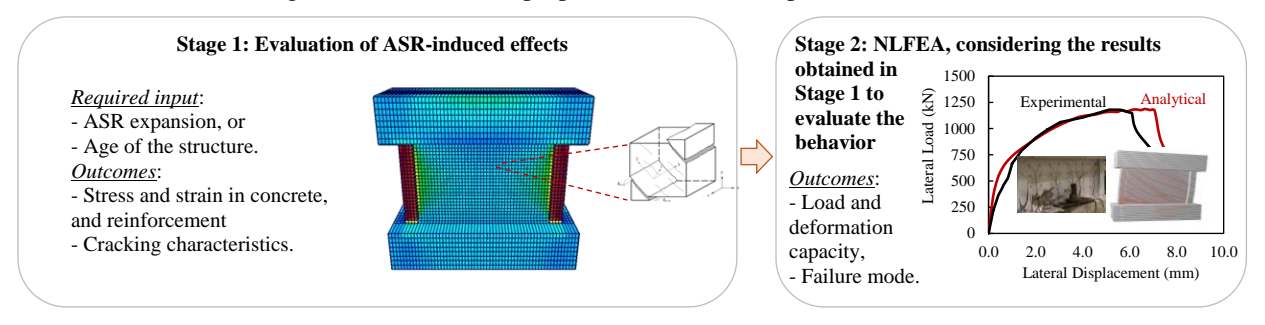


Figure 11 - Two-stage analysis procedure for the assessment of ASR-affected members

The compatibility relationship for concrete was modified to accommodate for the anisotropic expansion due to ASR, which is treated as an elastic strain offset. The ASR-induced strains are evaluated for a stress condition representing the average long-term loading condition during which ASR expansion occurred; these strains and their orientations are then held constant and carried through subsequent analyses as elastic strain offsets in the prestrain vector $\{\varepsilon_c^o\}$. The strain offsets in the principal directions $(\varepsilon_{c1.ASR}^o, \varepsilon_{c2.ASR}^o, \varepsilon_{c3.ASR}^o)$ are determined according to one of the ASR constitutive models implemented in the software. If angle θ defines the orientation of the principal axes, the following relationships are used for transforming the strains to the x, y reference system:

$$\varepsilon_{cx,ASR}^o = \varepsilon_{c1,ASR}^o \frac{(1 + \cos 2\theta)}{2} + \varepsilon_{c2,ASR}^o \frac{(1 - \cos 2\theta)}{2}$$
(17)

$$\varepsilon_{cy.ASR}^o = \varepsilon_{c1.ASR}^o \frac{(1 - \cos 2\theta)}{2} + \varepsilon_{c2.ASR}^o \frac{(1 + \cos 2\theta)}{2}$$
(18)

$$\gamma_{cxv,ASR}^o = \varepsilon_{c1,ASR}^o \sin 2\theta - \varepsilon_{c2,ASR}^o \sin 2\theta \tag{19}$$

$$\varepsilon_{cz,ASR}^o = \varepsilon_{c3,ASR}^o \tag{20}$$

The ASR-induced strains are added to the total prestrain vector, $\{\varepsilon_c^o\}$, which is then used to calculate the pseudo-stress vector defined in Eq. (9). The solution is subsequently carried forward as previously discussed for the MCFT.

For the changes in the concrete mechanical properties, two isotropic options were initially made available: user-defined properties, or properties calculated based on the recommendations made by the Institution of Structural Engineers (1992), depending on the free expansion and the undamaged concrete strength at 28 days. The mechanical properties of ASR-affected concrete were, therefore, assumed to be uniform in all directions. Two additional options were subsequently implemented as part of work conducted by Ferche and Vecchio (2022): an anisotropic formulation and its corresponding simplified isotropic version. To account for anisotropy in the mechanical properties of concrete, the effects of ASR damage are quantified as a function of the aggregate's reactivity potential and the long-term stress state. Modification factors are introduced for each principal direction to adjust the concrete compressive strength, tensile strength, and modulus of elasticity. Notably, these factors in any given direction are evaluated while considering the strain and stress states along the other two orthogonal directions. This ensures a comprehensive representation of the stress conditions, distinguishing between stress-free, uniaxial, biaxial, and triaxial states.

The modification factors are applied to the baseline properties of undamaged concrete, including compressive strength, tensile strength, and modulus of elasticity. These baseline properties can be determined from material tests conducted on cores extracted from undamaged regions of a structure. In cases where core testing is not feasible, estimations can be made using the specified 28-day strength and the structure's age. By integrating empirically-determined anisotropic modification factors into smeared crack formulations, the extended version of MCFT provides a more refined approach to represent ASR damage. Validation studies were performed on ASR-affected panel, beam, and shear wall specimens to obtain an indication of the accuracy of the proposed modeling procedure.

The anisotropic model, validated using the Charlwood (1992) expansion model, aligned well with experimental results, offering less conservative predictions than its isotropic counterpart in panel tests (see Fig. 12). For ASR-affected shear walls, the methodology produced consistent results, although additional mechanisms such as ASR expansion effects, confinement modeling, and boundary condition representation played a significant role in the computed response. In shear-critical beams with minimum shear reinforcement, results from the anisotropic and isotropic models showed negligible differences due to the mitigating effects of transverse reinforcement on ASR-induced damage. The simpler Charlwood model for ASR expansion performed comparably to the more complex Saouma and Perotti (2006) model, offering a practical choice for structural analysis. These insights highlight the versatility and reliability of the MCFT-based approach in modeling ASR-affected concrete elements with a high degree of accuracy.

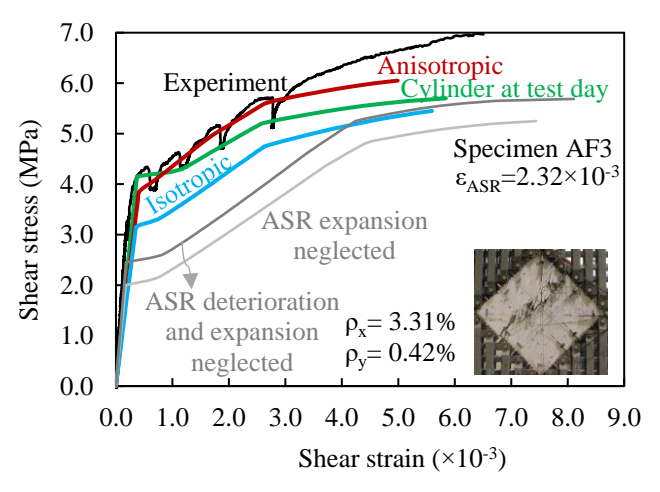


Figure 12 – Numerical versus experimental results for ASR-affected panel element (Ferche and Vecchio, 2022) (Note: 1 MPa = 0.145 ksi)

APPLICATION OF MCFT TO MODELING FRP-REPAIRED STRUCTURES

The repair and strengthening of deteriorated RC structures have emerged as critical areas of research, particularly in the context of aging infrastructure and increasing demands for sustainability. Among various strengthening methods, the use of fiber-reinforced polymer (FRP) composites has gained significant attention due to their high strength-toweight ratio, corrosion resistance, and ease of application. These advantages make FRP materials particularly attractive for addressing deficiencies caused by aging, seismic events, or design inadequacies. Numerous experimental and analytical studies have demonstrated the effectiveness of FRP in enhancing the performance of RC structures. However, modeling the behavior of FRP-repaired RC structures remains a challenging and evolving field, requiring accurate representation of complex mechanisms at both the component and system levels. At the component level, existing models have focused on capturing the interaction between FRP and concrete through bond-slip relationships (Sato and Vecchio, 2003), confinement enhancements (Lam and Teng, 2009), effects of FRP wraps on bar buckling (Karabinis et al. 2008), and cyclic strength degradation (Akguzel and Pampanin, 2012). While significant progress has been made in understanding the flexural behavior of FRP-repaired RC members, further work is needed to address their shear behavior, which remains less thoroughly investigated. At the system level, analyses of FRP-repaired RC structures are still limited (e.g., Eslami and Ronagh, 2013). The interactions between individual elements, the redistribution of forces, and the overall structural performance under seismic loading conditions require integrated approaches that link detailed local models with global behavior. Simplified modeling techniques, which rely on concentrated plastic hinges or calibrated member responses, are often used for practical modeling of the system-level behavior but they fail to account for critical mechanisms such as interfacial debonding between FRP and concrete or the cumulative effects of damage.

The application of MCFT to modeling FRP-repaired structures began more than 25 years ago and has evolved to address limitations in the literature, making valuable contributions to this field. One of the earliest studies, conducted by Vecchio and Bucci (1999), was FE analysis of FRP-repaired beams and slabs. They used plastic strain offsets coupled with element activation/deactivation to simulate the response of RC members prior to and after repair. Despite promising results, the model could not capture debonding failure because FRP sheets were represented as a smeared component within the concrete elements. Wong and Vecchio (2003) improved the model by discretely representing FRP sheets with truss elements and employing link elements to capture slippage at the bond interface. Sato and Vecchio (2003) further enhanced the analysis procedure by developing tension stiffening and crack formation models specifically for FRP-strengthened RC members, implementing them into the VecTor programs. Montoya et al. (2004) contributed by developing a new constitutive material model for concrete to account for the confinement effects of FRP wraps in axially loaded members. More recently, Sadeghian et al. (2019) developed a multi-platform simulation framework that extends the analysis procedure from the component-level to the system-level, enabling the modeling of interactions between repaired and non-repaired members, including force redistributions within the system.

The following section provides an overview of these advancements, highlighting key aspects of modeling FRP-repaired RC structures in the VecTor programs.

Modeling methodology

Cover spalling prior to repair - Axially loaded RC members subjected to cyclic loads may exhibit softening behavior before reaching the ultimate stress specified in their constitutive models. This behavior begins with the spalling of the concrete cover and continues as the longitudinal reinforcement starts to buckle. To capture this behavior, a cover spalling criterion was applied, where if the angle between the crack and the longitudinal reinforcement (α) is less than 30 degrees, the principal net compressive strain is limited to -3.5×10⁻³ mm/mm and the crack width (w_{cr}) is restricted to 2.0 mm (0.079 in.). If an element in the concrete cover zone (see Figure 13(a)) reaches one of these limits, it will be deactivated, meaning its strength and stiffness will be reduced to nearly zero. This approach allows for a more accurate simulation of the structural response under cyclic loading, as it reflects the reduced load-carrying capacity of the cover zone due to spalling.

Bond-slip effects - The FRP sheets are represented using truss elements, with their cross-sectional areas determined based on the tributary area of each element, as well as the thickness and number of FRP layers. A tension-only material is assigned to these truss elements, exhibiting a linear-elastic behavior with the maximum tensile stress set to the rupture strength of the FRP and negligible stress in compression. To incorporate the effects of interfacial stresses between the concrete and FRP, as well as the debonding failure mechanism, the concrete elements are connected to the FRP elements using link elements. Each link element consists of a tangential and a normal spring where the stiffness of the normal spring is set to a very large value, while the stiffness of the tangential spring is determined based on the bond-slip model assigned to the element. The verification studies were conducted using a

bilinear bond-slip model based on the fracture energy of concrete, originally developed by Nakaba et al. (2001) and later improved by Sato and Vecchio (2003). Figure 13(b) illustrates the link element and the bilinear bond-slip model.

Crack formation and tension stiffening - Sato and Vecchio (2003) proposed models integrated with the MCFT formulations to estimate crack formation and tension stiffening effects for FRP-strengthened RC members. Unlike steel reinforcements, FRP sheets exhibit unique elastic properties, brittle bond characteristics, and a susceptibility to peeling, which necessitate specialized modeling approaches. The proposed models are based on the tension chord approach, which evaluates the equilibrium between tensile stresses in the concrete and the bond stresses at the interface. According to these models, a new crack forms when the tensile stress in the concrete at the midpoint between existing cracks reaches its tensile strength. The models integrate the bond-slip relationship between FRP and concrete to account for strain differences and stress distribution along the FRP sheet. The crack spacing is expressed as a function of the contributions of both steel reinforcements and FRP sheets. For FRP, the spacing depends on the sheet thickness, elastic modulus, and fracture energy. The equation for crack spacing considers the reinforcement ratio, principal stress direction, and local bond-slip relationships. Sato and Vecchio (2003) demonstrated that FRP sheets contribute to reducing crack spacing, thereby improving crack distribution and overall structural performance.

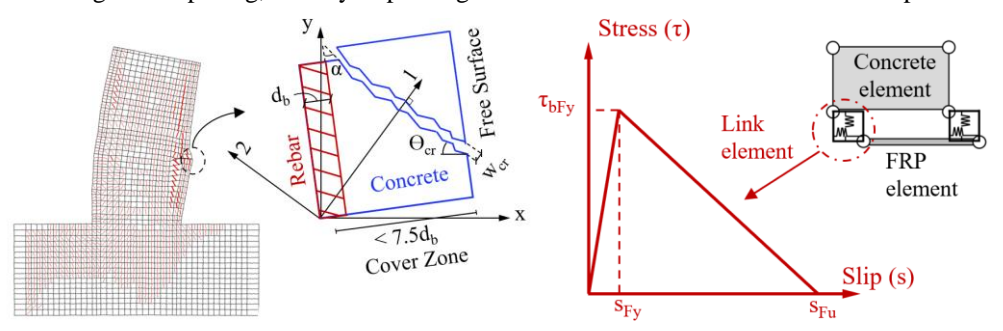


Figure 13 - (a) Schematic representation of spalling in the concrete cover zone and (b) bond-slip model assigned to link elements to compute interfacial stresses between concrete and FRP (Sadeghian, 2017)

Multi-platform simulation - Detailed FE modeling of an entire structural system, including FRP-repaired components, is often impractical due to the complexity of the analysis and high computational demands. Conversely, system-level analysis tools are unable to capture the intricate behavior of RC members confined with FRP. To overcome these challenges, Sadeghian et al. (2019) developed a multi-platform analysis framework, Cyrus, which integrates different analysis tools while ensuring full interaction between substructures. The coupled formulation of the analysis procedure enables consideration of force redistribution caused by stiffness changes across components. Furthermore, the integration module supports parallel processing, significantly reducing computational time and memory demands compared to traditional single-platform sequential analyses.

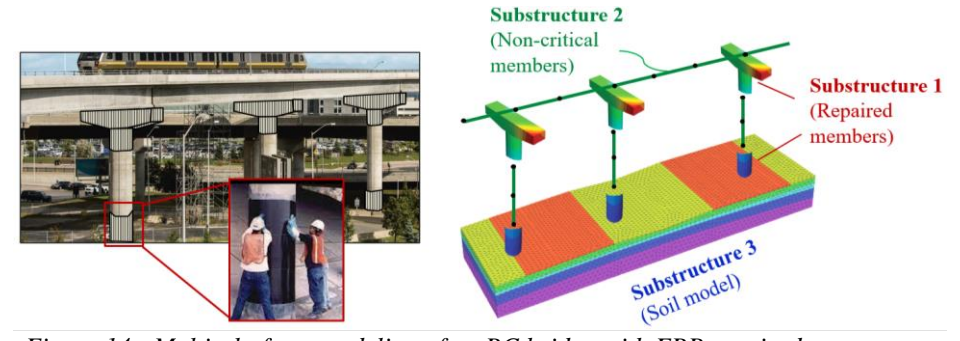


Figure 14 - Multi-platform modeling of an RC bridge with FRP repaired components

The proposed multi-platform analysis framework has been applied to various complex engineering problems including modeling RC structural systems with repaired components (see Fig. 14). In this framework, repaired members and other critical structural components are modeled using detailed FE programs, while non-critical parts of the structure are analyzed using computationally efficient frame-type software. To accurately connect different substructures, Sadeghian et al. (2018) introduced the F2M interface element which accounts for nonlinear stress distribution and transverse expansion at the interface. The framework supports multiple communication methods to exchange data (restoring force, stiffness, and displacement) between substructures including binary files, pipes, and TCP/IP sockets.

A standardized data exchange format developed by Huang et al. (2015) has been implemented into the framework, enabling seamless integration of substructures modeled in different analysis software.

Verification studies

The application of MCFT to RC structures with externally bonded FRP components has been verified at both the component and system levels in several studies. These include the modeling of FRP-strengthened shear-critical RC beams (Wong and Vecchio, 2003; Sato and Vecchio, 2003), axially loaded circular RC columns strengthened with CFRP wraps (Montoya et al. 2004), cyclically loaded square RC columns strengthened or repaired with GFRP wraps (Sadeghian, 2017), an RC frame with shear-critical beams repaired using FRP sheets (Sadeghian and Vecchio, 2016), and an FRP-strengthened RC frame with critical beam-column joints (Sadeghian et al., 2020). Here, an overview of one of the verification studies is presented to demonstrate the capabilities of the proposed modeling methodology.

Sadeghian (2017) employed the multi-platform simulation procedure to analyze a series of seismically deficient RC columns tested by Memon and Sheikh (2005). These specimens were strengthened or repaired with GFRP layers and subjected to a combination of constant axial load and reversed cyclic lateral load. The test parameters included the presence of initial damage in the specimens, the number of GFRP layers, and the level of axial load. As shown in Fig. 15, the multi-platform model consisted of two substructures: the critical part of the column repaired/strengthened with GFRP wraps was modeled in detail using VecTor2 according to the procedure discussed in the previous section. Meanwhile, the rest of the column, which was expected to exhibit linear elastic behavior, was modeled using VecTor5, a computationally efficient frame analysis tool. The two substructures were integrated using Cyrus to ensure compatibility and equilibrium conditions were satisfied through the entire structural member. Figure 16 compares the predicted load-deflection responses of the specimens with those reported from the test. Overall, the computed results showed good agreement with the experimentally observed behavior. The numerical model effectively captured the peak load, strength degradation, and pinching behavior. However, it slightly overestimated the peak load for specimens with multiple GFRP layers. This discrepancy was likely due to the potential slip between GFRP layers, or the reduced confinement enhancement caused by the arching effect in square columns, mechanisms that were not accounted for in the analysis. For further details on the modeling approach and the discussion of the results refer to Sadeghian (2017).

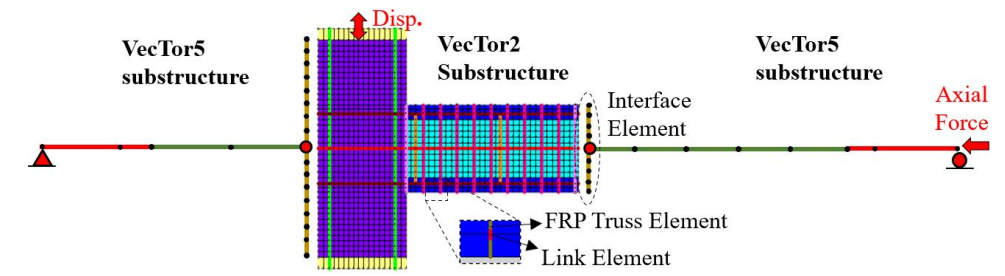


Figure 15 – Multi-platform model of RC columns strengthened with GFRP wraps (Sadeghian, 2017)

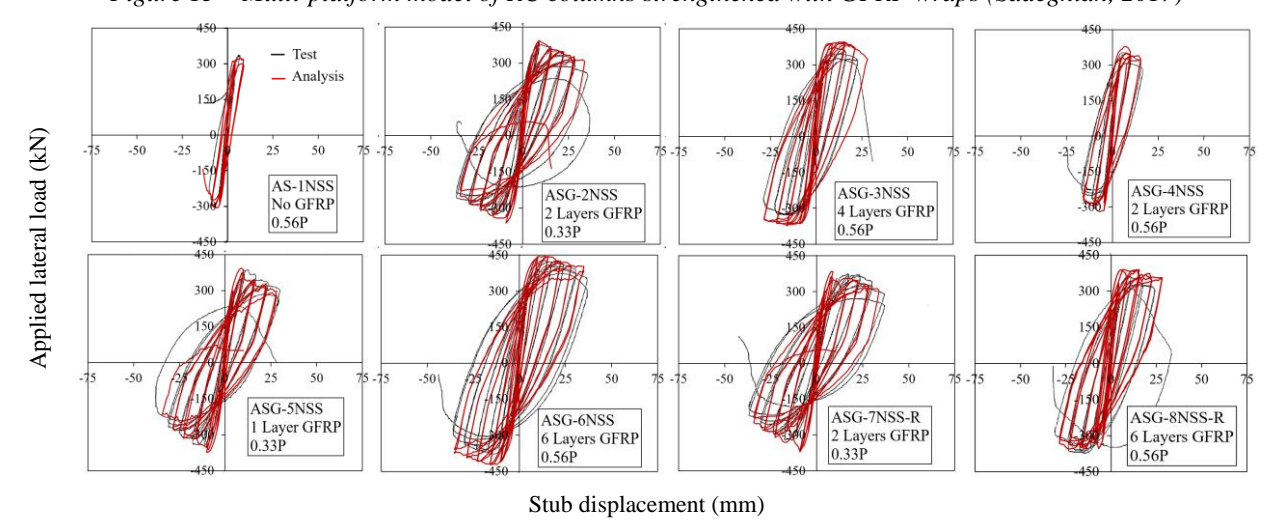


Figure 16 - Comparison of numerical and experimental reversed-cyclic load-deflection responses of RC columns strengthened with GFRP wraps (Sadeghian, 2017) (Note: 1.0 mm = 0.04 in., 1 kN = 0.225 kip.)

CONCLUSIONS

This paper underscores the enduring significance of the MCFT and the DSFM in advancing the modeling of concrete structures. Originally developed for newly designed structures, these methodologies have evolved to address challenges in assessing deteriorated and repaired RC structures. The incorporation of advanced features into MCFT has broadened its applicability, including the integration of nonlinear finite element analysis and stochastic methods. These enhancements allow for the evaluation of complex structural behaviors under diverse scenarios, including corrosion of the reinforcing steel, alkali-silica reaction, and fiber-reinforced polymer repairs. The findings demonstrate the robustness of MCFT and DSFM in accurately predicting structural responses, thereby supporting the development of effective assessment and rehabilitation strategies for aging infrastructure. The study highlights several key advancements:

- 1. Improved modeling of deterioration mechanisms, such as reinforcement corrosion and ASR, through detailed constitutive formulations and validation studies.
- Enhanced prediction capabilities for FRP-repaired structures by capturing critical interactions such as bondslip effects and confinement mechanisms.
- 3. Integration of stochastic analysis to address variability in material properties, which ensures a more comprehensive understanding of structural performance.

These developments not only validate the adaptability of MCFT but also emphasize its potential as a versatile tool for the civil engineering community. Moving forward, continued innovation in modeling techniques and computational frameworks will further refine the utility of MCFT, enabling more reliable and efficient solutions for the assessment and rehabilitation of concrete structures.

ACKNOWLEDGMENTS

The authors express their gratitude to Professor Frank Vecchio for his enduring contributions to the study of shear in concrete structures. The VecTor suite of analysis software, with its longevity and continuous improvement, stands out for its excellent ability to deliver accurate results without the need for calibration, and for its adaptability to new materials and structural problems.

REFERENCES

- AASHTO LRFD, 2024, "Bridge Design Specifications", 10th Edition, American Association of State Highway Transportation Officials (AASHTO), Washington, D.C., United States.
- ACI Code Committee 318, 2019, "Building Code Requirements for Reinforced Concrete (ACI 318-19) and Commentary", American Concrete Institute (ACI), Farmington Hills, Michigan, United States.
- Akguzel, U., and Pampanin, S., 2012, "Assessment and Design Procedure for the Seismic Retrofit of Reinforced Concrete Beam-Column Joints using FRP Composite Materials", ASCE J. Compos. Constr., 16(1).
- Alonso, C., Andrade, C., and Gonzalez, J.A., 1988, "Relation Between Resistivity and Corrosion Rate of Reinforcements in Carbonated Mortar Made with Several Cement Types", *Cement and Concrete Research*, 18(5), pp. 687-698.
- Bentz, E.C., Vecchio, F.J., and Collins, M.P., 2006, "The Simplified MCFT for Calculating the Shear Strength of Reinforced Concrete Elements", *ACI Structural Journal*, 103(4), pp. 614-624.
- Bentz, E.C., 2010, "Shear Strength of Beams and Implications of New Approaches", Technical Report, Fib Bulletin 57: Shear and Punching Shear in RC and FRC Elements, doi.org/10.35789/fib.BULL.0057.
- Cairns, J., Plizzari, G., Du, Y., Law, D., and Franzoni, C., 2005, Mechanical Properties of Corrosion-Damaged Reinforcement", *ACI Material Journal*, 102(4), 256-264.
- Collins, M.P., Quach, P.T., and Bentz, E.C., 2020, "Shear Behavior of Thick Slabs", *ACI Structural Journal*, 117(4), pp. 115-125.
- Charlwood, R.G., Solymar, Z.V., and Curtis, D.D., 1992, "A Review of Alkali Aggregate Reaction in Hydro Plants and Dams", *Proc. of the Int. Conf. of Alkali Aggregate Reactions in Hydroelectric Plants and Dams*, Fredericton, NB, Canada.
- Chung, L., Najm, H., Balaguru, P., 2008, "Flexural Behavior of Concrete Slabs with Corroded Bars", *Cement and Concrete Composites*, 30(3), pp.184-193.
- CSA Committee A23.3, 2024, "Design of Concrete Structures", Canadian Standards Association (CSA), Mississauga, ON, Canada, 301 pp.
- Eslami, A., and Ronagh, H.R., 2013, "Effect of FRP Wrapping in Seismic Performance of RC Buildings with and without Special Detailing A Case Study", *Compos. Part B: Eng. J.*, 45(1), pp. 1265-1274.

- Feng, Q., Visintin, P., and Oehlers, D.J., 2016, "Deterioration of Bond–Slip Due to Corrosion of Steel Reinforcement in Reinforced Concrete", *Magazine of Concrete Research*, 68(15), pp. 768-781.
- Ferche, A.C., Panesar, D.K., Sheikh, S.A., and Vecchio, F.J., 2017, "Toward Macro-modeling of ASR Affected Structures", *ACI Structural Journal*, 114(5), pp. 1121-1129. https://doi.org/10.14359/51700778.
- Ferche, A.C., and Vecchio, F.J., 2022, "Modeling of Alkali-Silica Reaction-Affected Shear-Critical Reinforced Concrete Structures", *ACI Structural Journal*, 119(2), pp. 75-88.
- Fib Bulletin No. 45, 2008, "Practitioners' Guide to FE Modelling of Reinforced Concrete Structures", International Federation for Structural Concrete (fib), Lausanne, Switzerland, doi.org/10.35789/fib.BULL.0045.
- Fib Commission 10, 2020, "The fib Model Code for Concrete Structures 2020", International Federation for Structural Concrete (fib), Lausanne, Switzerland.
- Guner, S., and Vecchio, F.J., 2010, "Pushover Analysis of Shear-Critical Frames: Formulation", *ACI Structural J.*, 107(1), pp. 63-71.
- Habibi, S., Ferche, A.C., and Vecchio, F.J., 2022, "Modeling Corrosion-Damaged Reinforced Concrete Members", *ACI Structural Journal*, 119(1), pp. 170-183.
- Huang, X., Sadeghian, V., Kwon, O.S., 2015, "Development of Integrated Framework for Distributed Multi-Platform Simulation", 6th Int. Conf. on Advances in Experimental Structural Eng., Urbana-Champaign, United States.
- Hunter, M.D., Ferche, A.C., and Vecchio, F.J., 2021a, "Stochastic Finite Element Analysis of Shear-Critical Concrete Structures", *ACI Structural Journal*, 118(3), pp. 71-83.
- Hunter, M.D., Ferche, A.C., and Vecchio, F.J., 2021b, "Influence of Spatial Variability of Concrete in Large Shear-Critical Structures", *ACI Structural Journal*, 118(2), pp. 249-262.
- Institution of Structural Engineers (ISE), 1992, "Structural Effects of Alkali-Silica Reaction," SETO, London, UK. Karabinis, A.I., Rousakis, T.C., Manolitsi, G.E., 2008, "3D Finite-Element Analysis of Substandard RC Columns Strengthened by Fiber-Reinforced Polymer Sheets", *ASCE J. Compos. Constr.*, 12(5), pp. 531-540.
- Kashani, M.M., Maddocks, J., and Dizaj. E.F., 2019, "Residual Capacity of Corroded Reinforced Concrete Bridge Components: State-of-the-Art Review", *ASCE Journal of Bridge Engineering*, 24(7).
- Lam, L., and Teng, J., 2009, "Stress-Strain Model for FRP-Confined Concrete under Cyclic Axial Compression", *Eng. Struct.*, 31(2), pp. 308–321.
- Liu, T., and Weyers, R.W., 1998, "Modeling the Dynamic Corrosion Process in Chloride Contaminated Concrete Structures", *Cement and Concrete Research*, 28(3), pp. 365-379.
- Ma, R.L., 2018, "Program Sherlock: A Tool for Stochastic Finite Element Analysis and Field Assessment of Concrete Structures", MSc Thesis, University of Toronto, Toronto, Canada, 140 pp.
- Maaddawy, T., Soudki, K., and Topper, T., 2005, "Long-term Performance of Corrosion-damaged Reinforced Concrete Beams", *ACI Structural Journal*, 102(5), pp. 649-656.
- Memon, M.S., and Sheikh, S., 2005, "Seismic Resistance of Square Concrete Columns Retrofitted with Glass Fiber-Reinforced Polymer", *ACI Structural Journal*, 102(5), pp. 774-783.
- Mitchell, D., and Collins, M.P., 1974, "Diagonal Compression Field Theory-A Rational Model for Structural Concrete in Pure Torsion", *ACI Journal Proceedings*, 71(8), pp. 396-408.
- Montoya, E., Vecchio, F.J., and Sheikh, S.A., 2004, "Numerical Evaluation of the Behaviour of Steel- and FRP-Confined Concrete Using Compression Field Modeling", *Engineering Structures*, 26(11), pp. 1535-1545.
- Nakaba, K., Kanakubo, T., Furuta, T., and Yoshizawa, H., 2001, "Bond Behavior Between Fiber-Reinforced Polymer Laminates and Concrete", *ACI Structural Journal*, 98(3), pp. 359-367.
- Pantazopoulou, S.J., and Papoulia, K.D., 2001, "Modeling Cover-Cracking Due to Reinforcement Corrosion in RC Structures", *Journal of Engineering Mechanics*, 127(4), pp. 342-351.
- Sadeghian, V., 2017, "A Framework for Multi-Platform Analytical and Experimental Simulations of Reinforced Concrete Structures", PhD Thesis, University of Toronto, Toronto, ON, Canada.
- Sadeghian, V., and Vecchio, F.J., 2018, "The Modified Compression Field Theory: Then and Now", *ACI Special Publication SP-328*, pp. 41-60.
- Sadeghian, V., Kwon, O.S., and Vecchio, F.J., 2019, "A Framework for Multi-Platform Simulation of Reinforced Concrete Structures", *Engineering Structures*, 181, pp.260-270. https://doi.org/10.1016/j.engstruct.2018.12.023.
- Sadeghian, V., Kwon, O.S., and Vecchio, F.J., 2018, "Modelling Beam-Membrane Interface in Reinforced Concrete Frames", *ACI Structural Journal*, 115(3), pp. 826-836.
- Sadeghian, V., and Vecchio, F.J., 2016, "Application of Multi-Scale Modelling on Large Shear-Critical Reinforced Concrete Structural Systems Repaired with FRP Sheets", *Innovations in Corrosion and Materials Science*, 6(2), pp. 106-114.

- Sadeghian, V., Tanyous, M., and Mirshekar, M., 2020, "Modelling FRP-Strengthened Beam-Column Joints in Performance Assessment of RC Frames," 6th Int. Conf. on Construction Materials, Fukuoka, Japan.
- Saouma, V., and Perotti, L., 2006, "Constitutive Model for Alkali-Aggregate Reactions", *ACI Materials Journal*, 103(3), pp. 194-202.
- Sato, Y., and Vecchio, F.J., 2003, "Tension Stiffening and Crack Formation in Reinforced Concrete Members with Fiber-Reinforced Polymer Sheets", *ASCE Journal of Structural Engineering*, 129(6), pp. 717-724.
- Stewart, M.G., and Al-Harthy, A., 2008, "Pitting Corrosion and Structural Reliability of Corroding RC Structures: Experimental Data and Probabilistic Analysis", *Reliability Engineering and System Safety*, 93, pp. 373-382.
- Vecchio, F.J., 2001, "Disturbed Stress Field Model for Reinforced Concrete: Implementation", *ASCE Journal of Structural Engineering*, 127(1), pp. 12-20.
- Vecchio, F.J., 2001, "Non-linear Finite Element Analysis of Reinforced Concrete: At the Crossroads?", *Structural Concrete*. 2(4), pp. 201-212.
- Vecchio, F.J., Lai, D., Shim, W., and Ng, J. 2001, "Disturbed Stress Field Model for Reinforced Concrete: Validation", ASCE Journal of Structural Engineering, 127(4), pp. 350-358.
- Vecchio, F.J., and Bucci, F., 1999, "Analysis of Repaired Reinforced Concrete Structures", *ASCE J. of Structural Engineering*, 125(6), pp. 644-652.
- Vecchio, F.J., and Collins, M.P., 1986, "The Modified Compression Field Theory for Reinforced Concrete Elements Subjected to Shear", *ACI Journal*, pp. 219-231.
- Wagner, H., 1929, "Ebene Blechwandtra" ger mit sehr du"nnem Stegblech", Z. Flugtech. Motorluftschiffahrt, Berlin, Germany, V. 20, No. 8-12.
- Wang, X.H., and Liu, X.L., 2004, "Modelling Effects of Corrosion on Cover Cracking and Bond in Reinforced Concrete", *Magazine of Concrete Research*, 56(4), pp. 191-199.
- Wong, P.S., Trommels, H., and Vecchio, F.J., 2013, "VecTor2 and FormWorks User's Manual", 2nd Edition, Department of Civil Engineering, University of Toronto, Toronto, Canada, 311 pp.
- Wong, R.S.Y., and Vecchio, F.J., 2003, "Towards Modeling of Reinforced Concrete Members with Externally-Bonded FRP Composites", *ACI Structural Journal*, 100(1), pp. 47-55.
- Zaborac, J., Athanasiou, A., Salamone, S., Bayrak, O., and Hrynyk, T., 2019, "Evaluation of Structural Cracking in Concrete", Technical Report 0-6919-1, Center for Transportation Research, Uni. of Texas at Austin, Austin, TX, United States.

AUTHOR BIOS

Anca Ferche is an Assistant Professor in the Department of Civil, Architectural and Environmental Engineering at The University of Texas at Austin, Austin, Texas. She earned her MASc and PhD degrees from the University of Toronto, Canada, under the mentorship of Prof. Frank Vecchio, whose guidance greatly influenced her technical expertise and research philosophy. Her research interests span the performance assessment of reinforced concrete structures, concrete deterioration mechanisms, and the rehabilitation of structures.

Vahid Sadeghian is an Associate Professor in the Department of Civil and Environmental Engineering at Carleton University, Canada. His research focuses on enhancing the performance of concrete structures through the development of advanced analysis methods, as well as the application of innovative materials and construction techniques. He had the privilege of working under the supervision of Prof. Frank Vecchio during his MASc and PhD studies, whose mentorship has profoundly shaped both his technical expertise and personal growth.